

Original Article

Anticancer bioactive peptides suppress human colorectal tumor cell growth and induce apoptosis via modulating the PARP-p53-Mcl-1 signaling pathway

Li-ya SU^{1, #}, Ying-xu SHI^{1, #}, Mei-rong YAN¹, Yaguang XI², Xiu-lan SU^{1, *}

¹Clinical Medicine Research Center of the Affiliated Hospital, Inner Mongolia Medical University, Hohhot 010050, China; ²University of South Alabama Mitchell Cancer Institute, Mobile, AL 36604, USA

Aim: We have reported novel anticancer bioactive peptides (ACBPs) that show tumor-suppressive activities in human gastric cancer, leukemia, nasopharyngeal cancer, and gallbladder cancer. In this study, we investigated the effects of ACBPs on human colorectal cancer and the underlying mechanisms.

Methods: Cell growth and apoptosis of human colorectal tumor cell line HCT116 were measured using cell proliferation assay and flow cytometry, respectively. The expression levels of PARP, p53 and Mcl1A were assessed with Western blotting and immunohistochemistry. For evaluation of the *in vivo* antitumor activity of ACBPs, HCT116 xenograft nude mice were treated with ACBPs (35 µg/mL, ip) for 10 days.

Results: Treatment of HCT116 cells with ACBPs (35 µg/mL) for 4–6 days significantly inhibited the cell growth. Furthermore, treatment of HCT116 cells with ACBPs (35 µg/mL) for 6–12 h significantly enhanced UV-induced apoptosis, increased the expression of PARP and p53, and decreased the expression of Mcl-1. Administration of ACBPs did not change the body weight of HCT116 xenograft nude mice, but decreased the tumor growth by approximately 43%, and increased the expression of PARP and p53, and decreased the expression of Mcl-1 in xenograft mouse tumor tissues.

Conclusion: Administration of ACBPs inhibits human colorectal tumor cell growth and induces apoptosis *in vitro* and *in vivo* through modulating the PARP-p53-Mcl-1 signaling pathway.

Keywords: anticancer bioactive peptides; colorectal cancer; HCT116 cells; apoptosis; p53; Mcl-1; PARP

Acta Pharmacologica Sinica (2015) 36: 1514–1519; doi: 10.1038/aps.2015.80; published online 23 Nov 2015

Introduction

Colorectal cancer is one of the most common human cancers and one of the major causes of cancer-related deaths^[1, 2]. Surgery is still considered to be the first option for colorectal cancer treatment, especially for patients in the early stages of the disease. However, approximately 50% of colorectal cancer cases recur, and the tumor often undergoes metastasis after surgery, which may be attributable to a failure to find occult metastases or to achieve complete resection of the lesion^[3]. Surgery combined with radiotherapy and chemotherapy has been shown to improve the five-year survival rate of patients significantly, but the toxicity and side effects of these therapies

are of concern for improving the overall quality of patient survival^[4]. Therefore, novel, more efficacious, and safer therapeutics are required in clinical settings to improve the management of colorectal cancer.

Bioactive peptides are isolated from animals, plants, or microorganisms and are usually easily digested and absorbed^[5]. These peptides exhibit a variety of metabolic and physiological functions in humans. For example, some are able to lower blood pressure and promote nerve cell differentiation, which may be due to their hypolipidemic, anti-oxidative, antibacterial, and antiviral properties^[6]. We extracted novel anticancer bioactive peptides (ACBPs) from goat spleens after they had been immunized with human gastric cancer extracts^[7]. Our previous studies showed that ACBPs significantly and effectively inhibited tumor cell proliferation in gastric cancer, leukemia, nasopharyngeal cancer, and gallbladder cancer^[7–10]. In this study, we found that ACBPs significantly inhibited the

[#] These authors contributed equally to this work.

^{*} To whom correspondence should be addressed.

E-mail xlsu@hotmail.com

Received 2015-05-31 Accepted 2015-08-12

growth of and induced apoptosis in human colorectal cancer HCT116 cells. The mechanism by which ACBPs induce apoptosis is through the upregulation of PARP and p53 and the downregulation of Mcl-1. The anticancer activity of ACBPs was also validated in a xenograft animal model. Therefore, our results support that ACBPs are novel anticancer agents that inhibit colorectal tumor cell growth and induce apoptosis by regulating PARP-p53-Mcl-1 signaling.

Materials and methods

Production and purification of ACBPs

ACBPs were prepared and purified as previously reported^[7]. A concentration of 35 µg/mL was adapted for the treatment of cells throughout the study.

Cell culture

HCT116 cells were purchased from the American Type Culture Collection (ATCC, Manassas, VA, USA). Cells were maintained in IMDM culture medium (Invitrogen, Grand Island, NY, USA) that was supplemented with 10% heat-inactivated fetal bovine serum (FBS; TBD Science, China), 100 U/mL penicillin, and 100 U/mL streptomycin. HCT116 cells were cultured in a humidified atmosphere of 5% CO₂ at 37 °C.

Cell proliferation assay

Cells were seeded at a density of 1000 cells per well in 96-well plates containing IMDM with 10% FBS. Cells treated with ACBPs (35 µg/mL) or a control vehicle were measured once daily for 6 d. For the CCK-8 assay (Dojindo Molecular Technologies, Beijing, China), we followed the manufacturer's instructions. In brief, after adding 10 µL of CCK-8 solution to each well, cells seeded in the 96-well plate were incubated for 2 h at 37 °C and then examined at 450 nm with an ELISA plate reader.

Flow cytometry analysis

After having reached the logarithmic growth phase at a confluence of 70% to 80%, the cells were treated with ACBP (35 µg/mL) combined with 40 J/m² UV to induce apoptosis. At the indicated time points (1, 2, 3, 4, 5, and 6 h), groups of cells were treated with 0.25% trypsin-EDTA at 37 °C for 5 min and then collected and fixed with 75% ethanol overnight at 4 °C. The fixed cells were stained with 50 µg/mL propidium iodide (PI) and 50 µg/mL RNase A in PBS for 20 min at 37 °C. The DNA content of approximately 10000 cells was analyzed with a COULTER flow cytometer (EPICS-XL) and EXPO32-ADC software. The percentage of apoptotic cells (expressed as the percentage of the total number of cells) was also analyzed with the EXPO32-ADC software, and the results were presented in bar charts (prepared in Microsoft Excel).

Western blot analysis

Cells were lysed in 1× SDS-PAGE sample buffer, and the total protein was quantified using the BCA protein assay reagent (Thermo Fisher, Grand Island, NY, USA). The cell lysates were loaded onto a 12% SDS-PAGE gel and separated and

then electrophoretically transferred to a polyvinylidene fluoride membrane. The membrane was blocked in a 5% skim milk suspension for 1 h at room temperature prior to an overnight incubation at 4 °C with one of the following primary antibodies: anti-poly (ADP-ribose) polymerase (PARP) (CST, Shanghai, China), anti-p53 (MBL, Woburn, MA, USA), anti-Mcl-1 (Santa Cruz Biotechnology, Santa Cruz, CA, USA), anti-p53 upregulated modulator of apoptosis (PUMA) (CST) or anti-GAPDH (Santa Cruz Biotechnology). The membrane was subsequently incubated with the anti-rabbit or anti-mouse HRP-IgG (Santa Cruz Biotechnology) secondary antibody for 1 h at room temperature. Chemiluminescence was detected with an ECL blot detection system (Santa Cruz Biotechnology).

Xenograft model and treatment

Eight-week-old athymic nude male mice (BALB/c *nu/nu*; Institute of Laboratory Animal Sciences, Chinese Academy of Medical Sciences, Beijing, China) were housed in a sterile animal facility and subcutaneously inoculated with HCT116 cells (1×10⁷) in 0.1 mL PBS. The protocol for the treatment of the animals was reviewed and approved by our ethics committee. All mice developed single palpable tumors within one week after inoculation. The mice were randomly divided into control (*n*=5) and ACBP-treated (*n*=6) groups. A dose of 0.5 mL ACBPs (35 µg/mL) was administered daily via intraperitoneal injection in the treatment group, whereas the control mice were injected with 0.5 mL of normal saline (NS) solution. The mice were euthanized after 10 d of treatment. The tumors, livers, and spleens were collected, weighed, and dissected. Portions of each tissue were fixed in formalin and embedded in paraffin. Tissue sections were stained with hematoxylin and eosin (HE).

Immunohistochemistry

Paraffin-embedded tissues were sectioned to a thickness of 4 µm and stained with HE, or immunohistochemistry (IHC) was carried out. The IHC protocol was modified based on the manual of the S-P Hypersensitive Kit (Maixin Biological Technology Development Co, Fuzhou, China). Antigen retrieval after deparaffinization was carried out by placing the samples in a microwave oven for 10 min. We used rabbit anti-human PARP (ab6079), rabbit anti-human PUMA (bs1573R), and rabbit anti-human Mcl-1 (bs1352R) antibodies obtained from the Biosynthesis Biotechnology Co (Beijing, China). The rabbit anti-p53 (MAB-0142) antibody, the S-P Hypersensitive Kit (mouse and rabbit; 812059710), and the 3,3'-diaminobenzidine (DAB) reagents (806180031) were obtained from the Maixin Biological Technology Co. Sections were stained with DAB, counterstained with HE, dehydrated in xylene, and mounted. After immunohistochemical staining, the samples were observed under a light microscope (Olympus, Tokyo, Japan), and the results were quantified using the Olympus CX41 Image Analysis System.

Statistical analysis

The data are presented as the mean±standard deviation (SD).

Statistical analyses were performed using *t*-tests for two groups; $P < 0.05$ was considered to be statistically significant. All statistical analyses were performed using the SPSS (Statistical Package for the Social Sciences) program (version 13.0).

Results

ACBPs inhibit the growth of HCT116 colorectal tumor cells *in vitro* in a time-dependent manner

To quantify the inhibitory effect of ACBPs on cell growth, human colorectal tumor HCT116 cells were treated with either ACBPs (35 $\mu\text{g}/\text{mL}$) or vehicle controls. The CCK-8 assay was employed to measure cell growth once daily over a period of 6 d. Our results showed that ACBPs significantly suppressed the growth of HCT116 cells and that their inhibitory effects are time-dependent (Figure 1).

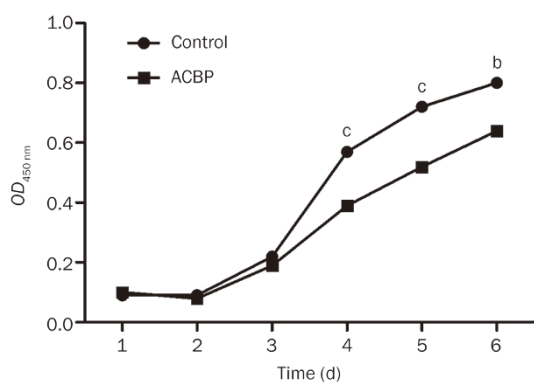


Figure 1. ACBPs inhibit the growth of human colorectal tumor HCT116 cells. Cells were seeded at a density of 1000 cells/well in 96-well plates in IMDM medium with 10% FBS. The absorbance at 450 nm was measured for the CCK-8 assay. The results are presented as the mean \pm SD of three independent experiments. ^b $P < 0.05$, ^c $P < 0.01$.

ACBPs induce apoptosis in HCT116 cells

The ACBP-induced apoptosis of HCT116 cells was also quantified by Annexin V-FITC/PI staining and flow cytometry. Our results showed that the treatment of HCT116 cells with ACBPs at 35 $\mu\text{g}/\text{mL}$ enhanced apoptosis that was induced by UV (40 J/m^2) exposure (Figure 2A and 2B). To study the molecular mechanisms underlying the ability of ACBPs to enhance UV-induced apoptosis in HCT116 cells, we examined the expression of PARP, p53, Mcl-1, and PUMA, respectively. As shown in Figure 2C, ACBP treatment after 24 h resulted in increased PARP and p53 expression but decreased Mcl-1 expression. However, the expression of PUMA remained unchanged. These results were consistent with the time-dependent effects of ACBPs on HCT116 cells that were observed after UV stimulation.

ACBPs suppress xenograft tumor growth *in vivo*

A xenograft nude mouse model was used to test the biological activity of ACBPs *in vivo*, and mice were inoculated with HCT116 cancer cells. Our results suggest that ACBP treatment improved the survival animals when compared with the con-

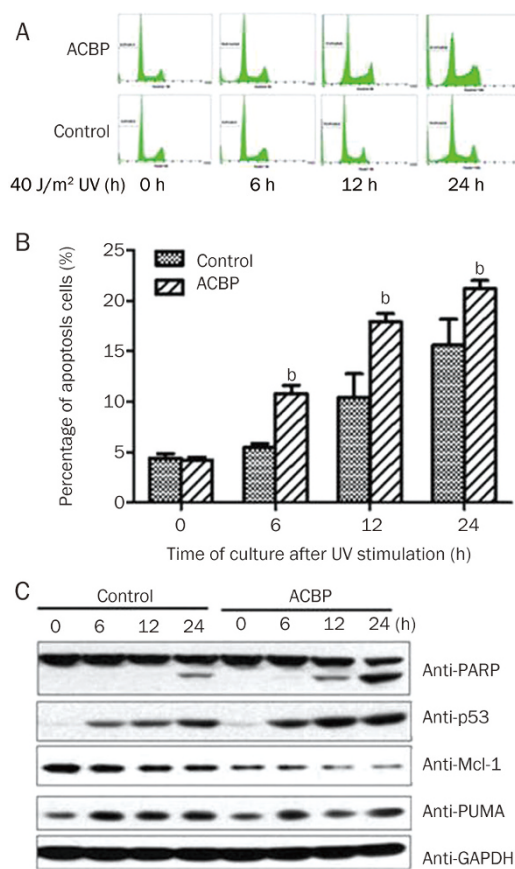


Figure 2. (A) ACBPs promote UV-induced cell apoptosis. PI was incorporated into the FACS assay to analyze apoptosis in HCT116 cells treated with ACBPs (35 $\mu\text{g}/\text{mL}$) after UV irradiation. (B) Bar graph showing the percentage of apoptosis (^b $P < 0.05$). The error bars represent the standard deviations (SD). (C) Expression of PARP, p53, Mcl-1, and PUMA in response to ACBP treatment at 35 $\mu\text{g}/\text{mL}$ in HCT116 cells.

rol group. The mice in the treatment group were more active and had better appetites, and they resembled normal mice in appearance and body weight. At the end of the experiment, tumors were harvested, and the tumor weights of all groups were examined. Compared with the control group, ACBP treatment significantly suppressed tumor growth by approximately 43% (Figure 3A). The body weights of the ACBP-treated mice were not changed compared to those in the control, whereas the tumor weights of ACBP-treated mice were lower than the tumor weights of the control mice, although the values were not significantly different (Figure 3B). Liver weights and liver indices did not differ between the two groups (Figure 3C). In addition, The spleen weight of the ACBP-treated mice was not changed compared to those in the control, but the spleen weight ratio (%) was significantly lower compared with the controls ($P = 0.0015$; Figure 3D). Cell cycle progression and the apoptosis of the tumor cells in the different groups were examined by flow cytometry. ACBP treatment resulted in a higher incidence of apoptosis compared with the control, but the effects were not significant (Figure 3E). The cell cycle analysis indicated that ACBPs promoted

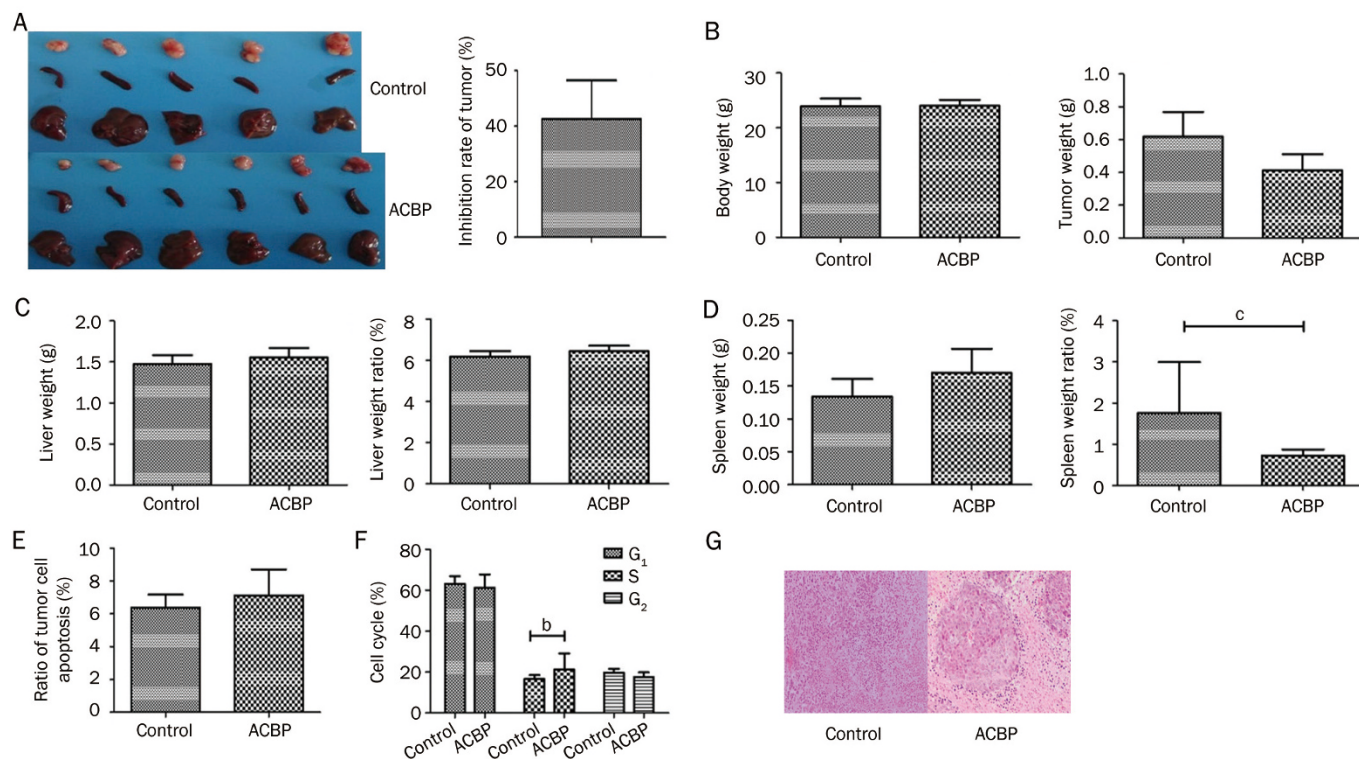


Figure 3. ACBPs suppress tumor growth *in vivo*. Tumors were harvested after treatment with ACBPs ($n=6$) and were compared with the control ($n=5$), with an average inhibitory rate of 43% (A). Body and tumor weight (B), liver weight (C) were measured, the differences between two groups were not statistically significant. Whereas the spleen indices were significantly lower than that in the control ($^cP<0.01$, D). Analysis of tumor apoptosis by flow cytometry *in vivo*. The tumor cell apoptosis rate was higher in the ACBP-treated group, but the difference was not statistically significant (E). Analysis of tumor cell cycle by flow cytometry *in vivo*. The proportion of cells that entered the cell cycle was higher in the ACBP-treated group than that in the control group ($^bP<0.05$, F). HE staining of tumor specimens harvested from *in vivo* experiments. More tumor cells with apoptotic features were detected in the ACBP-treated group (G).

the entry of tumor cells into the S phase of the cell cycle and that the results were statistically significant ($P<0.05$; Figure 3F). HE staining showed that the tumors in the xenograft mice treated with ACBPs contained more cells that exhibited the characteristics of apoptosis than the controls (Figure 3G).

ACBPs induce molecules that promote cell apoptosis *in vivo*

We evaluated the expression levels of PARP, p53, Mcl-1, and PUMA in tissues of the xenograft mice by immunohistochemistry. As shown in Figure 4, the expression of PARP appeared to be higher in ACBP-treated mice, but no significant difference was found compared with the control group ($P=0.136$). However, p53 was significantly upregulated ($P=0.025$), whereas Mcl-1 expression was dramatically decreased ($P=0.003$) in the ACBP-treated group compared with the control group. Consistent with the *in vitro* data, PUMA did not appear to be altered in either of the groups ($P=0.671$).

Discussion

ACBPs were isolated by our group from the spleens of goats that had been immunized with human gastric cancer extracts. Our previous study found that ACBPs had a remarkable ability to inhibit human gastric cancer growth both *in vitro* and *in vivo*^[11].

In addition, ACBPs were found to sensitize tumor cells to cisplatin^[12]. However, the mechanisms responsible for the anticancer activity of the ACBPs remain undiscovered. In this study, we used human colorectal tumor cell line, HCT116, as a research model to study the interaction of ACBPs with the genes that are involved in apoptosis.

Members of the caspase (cysteiny l aspartate-specific protease) family play a significant role in apoptosis^[13]. PARP is the target of caspase-3^[14]. When PARP is cleaved by caspase-3, Ca^{2+}/Mg^{2+} -dependent endonuclease activity will be increased to degrade microsomal DNA, initiating apoptosis^[15]. The role of p53 in apoptosis has been extensively reported, and it is known to bind to the Bcl-2 protein in the cytoplasm. The Bcl-2 family consists of highly homologous proteins that can be divided into anti-apoptotic (Bcl-2, Bcl-xL, and Mcl-1) and pro-apoptotic (Bax, Bak, PUMA, Noxa, and Bim) members. Mcl-1 is a member of the Bcl-2 family that has a short half-life^[16]. Overexpression of Mcl-1 can support tumor cell survival^[17], but the mechanism by which Mcl-1 promotes cell survival remains unclear. Mcl-1 can also bind to Bim or Bak to form a heterodimer that inhibits the release of cytochrome *c* to block apoptosis^[18]. After cells receive apoptotic stimuli such as UV, intracellular p53 levels increase. Therefore, p53 can compete

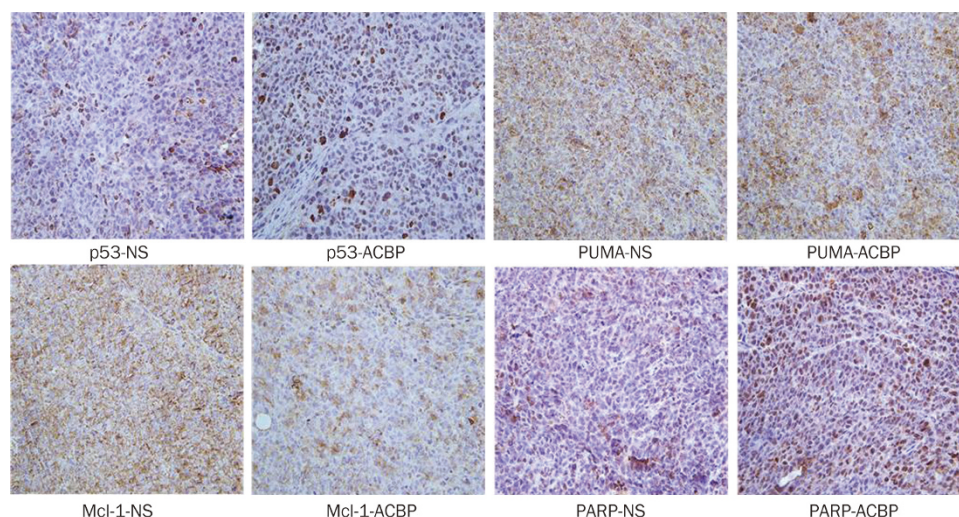


Figure 4. IHC analysis of p53, PUMA, Mcl-1, and PARP expression in xenograft mouse tumor tissues. Brown represents positive signals (400 \times).

with Bak to bind to Mcl-1 in the cytoplasm, leading to the release of additional Bak. Bak polymerization could increase the permeability of the mitochondrial outer membrane and ultimately induce mitochondrial apoptosis. Previous studies have demonstrated that PUMA can facilitate the binding of its BH3 domains to Bcl-2/Bcl-xL on the mitochondrial membrane to counteract the inhibitory function of Bcl-2/Bcl-xL on Bax/Bak^[19]. The increased mitochondrial membrane permeability due to changes in the conformation of Bax/Bak promote the release of cytochrome *c* and facilitate the formation of the apoptosis complex, which is composed of cytochrome *c*, ATP, and Apaf-1^[19]. In this study, we assessed how PARP, p53, Mcl-1, and PUMA are altered in response to ACBP treatment in *in vitro* and *in vivo* models.

First, our results showed that ACBPs significantly inhibited HCT116 cell growth *in vitro* and also enhanced UV-induced cell apoptosis. Western blotting analysis revealed that PARP and p53 were upregulated, whereas Mcl-1 was nearly absent when the cells were subjected to ACBP treatment. PARP is a DNA damage receptor that functions upstream of the p53 signaling pathway. Upregulation of PARP by radiation-induced DNA damage can induce p53, which in turn targets the Mcl-1 binding sites on Bak and/or Bax to release Mcl-1. Free Mcl-1 is susceptible to degradation. However, PUMA did not show any response to the ACBPs. Therefore, we hypothesize that the PARP-p53-Mcl-1 pathway may be involved in ACBP-induced apoptosis in HCT116 cells (Figure 5).

Second, we further investigated our *in vitro* findings using a xenograft animal model. We found that the average tumor size of the ACBP-treated mice was smaller than the average tumor size in the control group, which is likely to be responsible for the improved ability of the ACBP-treated mice to survive due to reduced tumor burdens. Cell cycle and apoptosis analyses indicated that ACBPs promoted the entry of tumor cells into the S phase. In addition, HE staining showed that apoptosis in tumor tissues resulted from ACBP treatment.

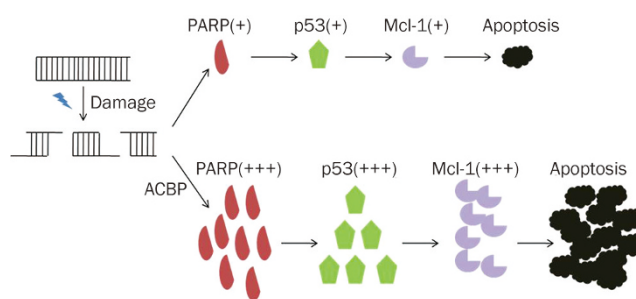


Figure 5. Mechanistic scheme outlining how ACBPs induce apoptosis.

Immunohistochemistry results indicated that PARP and p53 were overexpressed in xenograft tumor tissues from the ACBP-treated mice; however, PARP expression was not statistically different from the control group. In agreement with the *in vitro* results, Mcl-1 was dramatically decreased in tumor tissues subjected to ACBP treatment, but PUMA was not altered in either the ACBP-treated or control group.

In summary, our results demonstrate that ACBPs are novel anticancer agents for the treatment of colorectal cancer because they can effectively inhibit tumor growth and induce apoptosis. Our *in vitro* and *in vivo* findings suggest that PARP, p53, and Mcl-1 are involved in carrying out the apoptosis induced by ACBPs. These results provide novel insights into our understanding of the molecular mechanisms underlying the anticancer activity of ACBPs, which will allow the development of more efficacious and safer bioactive agents for use in control of colorectal cancer.

Acknowledgements

This research was supported by the National Natural Science Foundation of China (No 81160254 and 81450047).

Author contribution

Li-ya SU, Ying-xu SHI, and Xiu-lan SU designed the research; Li-ya SU, Ying-xu SHI, and Mei-rong YAN performed the studies; Li-ya SU and Ying-xu SHI analyzed the data; Li-ya SU, Ying-xu SHI, Yaguang Xi, and Xiu-lan SU wrote the paper.

References

- 1 Bencini L, Bernini M, Farsi M. Laparoscopic approach to gastrointestinal malignancies: toward the future with caution. *World J Gastroenterol* 2014; 20: 1777–89.
- 2 Ferlay J, Shin HR, Bray F, Forman D, Mathers C, Parkin DM. Estimates of worldwide burden of cancer in 2008: GLOBOCAN 2008. *Int J Cancer* 2010; 127: 2893–917.
- 3 Landmann RG, Weiser MR. Surgical management of locally advanced and locally recurrent colon cancer. *Clin Colon Rectal Surg* 2005; 18: 182–9.
- 4 Oliphant R, Nicholson GA, Horgan PG, Molloy RG, McMillan DC, Morrison DS, *et al*. Contribution of surgical specialization to improved colorectal cancer survival. *Br J Surg* 2013; 100: 1388–95.
- 5 Zambonino Infante JL, Cahu CL, Peres A. Partial substitution of di- and tripeptides for native proteins in sea bass diet improves *Dicentrarchus labrax* larval development. *J Nutr* 1997; 127: 608–14.
- 6 Pang G, Chen Q, Hu Z, Xie J. Bioactive peptides: absorption, utilization and functionality. *Food Sci* 2013; 34: 375–91. Chinese.
- 7 Su L, Xu G, Shen J, Tuo Y, Zhang X, Jia S, *et al*. Anticancer bioactive peptide suppresses human gastric cancer growth through modulation of apoptosis and the cell cycle. *Oncol Rep* 2010; 23: 3–9.
- 8 Hou J, Yan M, Rong Y, Jiao T, Su X. Effect of anticancer bioactive peptide on leukemia mice. *Acta Academiae Med Neimongol* 2004; 26: 3–6.
- 9 Zhao Y, Peng S, Su X. Effects of anti-cancer bioactive peptide on cell cycle in human nasopharyngeal carcinoma strain CNE. *Chin J Otorhinolaryngol Head Neck Surg* 2006; 41: 607–11.
- 10 Yun Q, Su X, Ouyang X. Analysis of gene expression pattern in gallbladder carcinoma cells treated by anti-cancer bioactive peptide (ACBP). *China Prac Med* 2009; 4: 10–2. Chinese.
- 11 Yu L, Yang L, An W, Su X. Anticancer bioactive peptide-3 inhibits human gastric cancer growth by suppressing gastric cancer stem cells. *J Cell Biochem* 2014; 115: 697–711.
- 12 Su X, Dong C, Zhang J, Su L, Wang X, Cui H, *et al*. Combination therapy of anti-cancer bioactive peptide with Cisplatin decreases chemotherapy dosing and toxicity to improve the quality of life in xenograft nude mice bearing human gastric cancer. *Cell Biosci* 2014; 4: 7.
- 13 Ghavami S, Hashemi M, Ande SR, Yeganeh B, Xiao W, Eshraghi M, *et al*. Apoptosis and cancer: mutations within caspase genes. *J Med Genet* 2009; 46: 497–510.
- 14 Chaitanya GV, Steven AJ, Babu PP. PARP-1 cleavage fragments: signatures of cell-death proteases in neurodegeneration. *Cell Commun Signal* 2010; 8: 31.
- 15 Gibson BA, Kraus WL. New insights into the molecular and cellular functions of poly(ADP-ribose) and PARPs. *Nat Rev Mol Cell Biol* 2012; 13: 411–24.
- 16 Stewart DP, Koss B, Bathina M, Perciavalle RM, Bisanz K, Opferman JT. Ubiquitin-independent degradation of antiapoptotic MCL-1. *Mol Cell Biol* 2010; 30: 3099–110.
- 17 Koss B, Morrison J, Perciavalle RM, Singh H, Rehg JE, Williams RT, *et al*. Requirement for antiapoptotic MCL-1 in the survival of BCR-ABL B-lineage acute lymphoblastic leukemia. *Blood* 2013; 122: 1587–98.
- 18 Bolesta E, Pfannenstiel LW, Demelash A, Lesniewski ML, Tobin M, Schlanger SE, *et al*. Inhibition of Mcl-1 promotes senescence in cancer cells: implications for preventing tumor growth and chemotherapy resistance. *Mol Cell Biol* 2012; 32: 1879–92.
- 19 Vela L, Gonzalo O, Naval J, Marzo I. Direct interaction of Bax and Bak proteins with Bcl-2 homology domain 3 (BH3)-only proteins in living cells revealed by fluorescence complementation. *J Biol Chem* 2013; 288: 4935–46.